Pergamon

Int. Comm. Heat Mass Transfer, Vol. 26, No. 7, pp. 945–954, 1999

0735-1933/99/$–see front matter

PII S0735-1933(99)00084-6

FREE CONVECTIVE STAGNATION-POINT FLOW IN A POROUS MEDIUM USING A THERMAL NONEQUILIBRIUM MODEL

D.A.S. Rees
Department of Mechanical Engineering, University of Bath,
Clavetrton Down. Bath. BA2 7AY. U.K.

I. Pop
Faculty of Mathematics. University of Cluj,R-3400 Cluj. CP 253. Romania

(Communicated by J.P. Hartnett and W.J. Minkowycz)

ABSTRACT

An analysis is made for the steady free convection boundary-layer flow near the stagnation point of a two-dimensional body which is embedded in a porous medium by adopting a two-temperature model of microscopic heat transfer. It is found that such a model modifies substantially the behaviour of the flow characteristics, particularly those of the heat transfer coefficients, and the region over which the thermal fields extend. © 1999 Elsevier Science Ltd

Introduction

Buoyancy-induced flows in fluid-saturated porous media is a branch of research undergoing rapid growth in the fluid mechanics and heat transfer characteristics of many engineering problems. Such problems, whose performance depend on a better understanding of convective flows in porous media, include geothermal systems, nuclear reactors, thermal insulations, drying processes, food stuffs etc. The growing volume of work devoted to this area is amply documented by the most recent reviews of Nield and Bejan [1], and Ingham and Pop [2]. However, most work on heat transfer in porous media has mainly been undertaken under the assumption that the convecting fluid and the porous medium are everywhere in local thermodynamic equilibrium, although in most practical applications the solid and fluid phases are not in equilibrium. Thermal nonequilibrium effects have been considered only a few times in the case of the Darcy-Bénard problem; see Combarnous [3] and Combarnous and Bories [4]. The reviews by Kuznetsov [5], and Vafai and Amiri [6] give detailed information about the research of the thermal nonequilibrium effects of the fluid flow through a porous packed bed. A very recent paper by Rees and Pop [7] discusses how the use of a two-temperature model of microscopic heat transfer modifies the classical Cheng and Minkowycz [8] vertical free convection boundary-layer flow.

The scope of the present is to discuss the effect of a two-temperature model on the free convection boundary-layer flow from a two-dimensional body of suitable shape immersed in a porous medium. We consider, for simplicity, the flow near a stagnation point, as this enables the governing equations to be much simplified and allows all the essential features to be clearly brought out. We follow the basic model for a vertical flat surface considered in [7]. We begin by considering the steady states, which are possible which for the geometrical configuration, are given by ordinary differential equations.

Basic Equations

We consider an infinite cylinder, which is embedded in a porous medium and mounted with its generators horizontal so that the flow is two-dimensional round the cylinder. The co-ordinate $\bar{x}$ measures distance round the cylinder and the coordinate $\bar{y}$ is in the perpendicular direction. It is assumed that the surface of the cylinder is held at the constant temperature T_w, while the ambient temperature is T_∞, where $T_w > T_\infty$. If we assume that Darcy's law holds, that the Boussinesq approximation is valid, but that the solid and fluid phases of the medium are not in equilibrium, then the equations governing the steady-state two-temperature flow model are, from Nield and Bejan [1] for example,

$$\frac{\partial \bar{u}}{\partial \bar{x}} + \frac{\partial \bar{v}}{\partial \bar{y}} = 0 \tag{1}$$

$$\frac{\partial \bar{u}}{\partial \bar{y}} - \frac{\partial \bar{v}}{\partial \bar{x}} = \frac{\rho_f g \beta K}{\mu} \frac{\partial T_f}{\partial \bar{y}} S(\bar{x}) \tag{2}$$

$$(\rho c)_f \left(\bar{u} \frac{\partial T_f}{\partial \bar{x}} + \bar{v} \frac{\partial T_f}{\partial \bar{y}} \right) = k_f \nabla^2 T_f + h(T_s - T_f) \tag{3}$$

$$0 = k_s \nabla^2 T_s - h(T_s - T_f) \tag{4}$$

Here $\bar{u}$ and $\bar{v}$ are the velocity components along the $\bar{x}$ and $\bar{y}$-axes, T is the temperature (where the f and s subscripts denote the fluid and solid phases, respectively), K is the permeability, g is the acceleration due to gravity, μ is the fluid viscosity, ρ is the density, c is the specific heat, β is the coefficient of the thermal expansion, k is the thermal conductivity, h is a coefficient which is used to model the microscopic transfer of heat between the fluid and solid phases and $S(\bar{x})$ is the sine of the angle between the outward normal from the body surface and the downward vertical.

Equations (1)-(4) may be nondimensionalized using the following transformations

$$(\bar{x},\bar{y}) = L(\hat{x},\hat{y}),\ (\bar{u},\bar{v}) = \frac{k_f}{(\rho c)_f L}(\hat{u},\hat{v}),\ (T_f, T_s) = (T_w - T_\infty)(\theta, \phi) + T_\infty, \tag{5}$$

where L is some length scale for the body. Further, we introduce a stream function $\hat{\psi}$ according to $\hat{u} = \partial\hat{\psi}/\partial\hat{y}$ and $\hat{v} = -\partial\hat{\psi}/\partial\hat{x}$. Equations (1)-(4) now become

$$\nabla^2\hat{\psi} = R\frac{\partial\theta}{\partial\hat{y}}S(\hat{x}),\ \nabla^2\theta = \hat{h}(\theta-\phi) + \frac{\partial\hat{\psi}}{\partial\hat{y}}\frac{\partial\theta}{\partial\hat{x}} - \frac{\partial\hat{\psi}}{\partial\hat{x}}\frac{\partial\theta}{\partial\hat{y}},\ \nabla^2\phi = \hat{h}\gamma(\phi-\theta) \tag{6}$$

where $\hat{h}$ and γ are dimensionless constants and R is the Darcy-Rayleigh number; these constants are defined as

$$\hat{h} = hL^2/\varepsilon k_f,\quad \gamma = k_f/k_s,\quad R = (\rho C)_f g\beta(T_w - T_\infty)K/\mu k_f \tag{7}$$

Let us now introduce the usual boundary-layer scaling

$$\hat{x} = x,\quad \hat{y} = R^{-1/2}y,\quad \hat{\psi} = R^{1/2}\psi \tag{8}$$

into Eqs. (6) to obtain

$$\frac{\partial^2\psi}{\partial y^2} = \frac{\partial\theta}{\partial y}S(x),\ \frac{\partial^2\theta}{\partial y^2} = H(\theta-\phi) + \frac{\partial\psi}{\partial y}\frac{\partial\theta}{\partial x} - \frac{\partial\psi}{\partial x}\frac{\partial\theta}{\partial y},\ \frac{\partial^2\phi}{\partial y^2} = H\gamma(\phi-\theta) \tag{9a, b, c}$$

where we have omitted terms, which are asymptotically small, compared with the retained terms as $R \to \infty$. In (9) H is defined according to

$$\hat{h} = RH \tag{10}$$

where $H = O(1)$ as $R \to \infty$. The boundary conditions are

$$\psi = 0,\ \theta = 1,\ \phi = 1 \text{ at } y = 0 \text{ and } \frac{\partial\psi}{\partial y}, \theta, \phi \to 0 \text{ as } y \to \infty \tag{11}$$

We note that these boundary conditions allow (9a) to be integrated once to yield

$$\frac{\partial\psi}{\partial y} = \theta\, S(x) \tag{12}$$

For stagnation-point flow we take

$$S(x) = x \tag{13}$$

and write

$$\psi = x\, f(y),\quad \theta = \theta(y),\quad \phi = \phi(y) \tag{14}$$

Using (14) in Eqs. (9b), (9c) and (12) leads to the following set of ordinary differential equations

$$f' = \theta,\quad \theta'' + f\theta' = H(\theta - \phi),\quad \phi'' = H\gamma(\phi - \theta) \tag{15a, b, c}$$

subject to the boundary conditions

$$f(0) = 0,\ f'(0) = 1,\ \phi(0) = 1 \text{ and } f', \phi \to 0 \text{ as } y \to \infty \tag{16}$$

where primes denote differentiation with respect to y.

The physical quantities of most interest are the fluid and solid phase Nusselt numbers, which are defined as

$$Nu_f = \frac{Lq_f}{k_f(T_w - T_\infty)}, \qquad Nu_s = \frac{Lq_s}{k_s(T_w - T_\infty)} \tag{17}$$

where $q_f = -k_f(\partial T_f/\partial \bar{y})_{\bar{y}=0}$ and $q_s = -k_s(\partial T_s/\partial \bar{y})_{\bar{y}=0}$. After some algebra, we obtain

$$Nu_f/R^{1/2} = -\theta'(0), \qquad Nu_s/R^{1/2} = -\phi'(0). \tag{18}$$

Numerical Solution

Equations (15) form an ordinary differential system with H and γ as the parameters. The easiest way to solve these equations for a wide range of values of H, say, is to use the Keller-box method. Although this method is normally used for parabolic systems of partial differential equations, we can adapt it by using H as the 'streamwise' variable and march forward for increasing or decreasing values of H to perform a parameter sweep. Other details of the method are well-known and the implementation used here has been described in detail in references [7] and [9]. In our computations we took 51 unequally spaced points in the y-direction with $0 \leq y \leq 1000$, and 201 values of H lying in the range $0.001 \leq H \leq 10$. Our numerical results are summarised in Fig. 1 where we display values of $\theta'(0)$ and $\phi'(0)$. When H is small there is a very substantial difference between the surface rates of heat transfer of the fluid and solid phases, indicating that nonequilibrium effects are strongest when H is small (this is consistent with the findings of [7] at small distances from the leading edge) which is not surprising since H is a measure of the ease with which heat is transferred between the phases. The numerical solutions also indicate that the thickness of the solid-phase temperature field increases as H decreases, which is consistent with the decreasing rate of heat transfer in that limit. Fig.1 also shows that the same qualitative effects are obtained as γ decreases. For larger values of H and as H increases, the inter-phase local heat transfer becomes more effective and this means that the difference between the solid and fluid temperature fields also decreases in magnitude. In the next section we show that this difference is proportional to H^{-1}.

Asymptotic Solution for Large Values of H

When H is large the form of Eqs. (15) suggests that the asymptotic analysis in this limit could very well be a singular perturbation problem. However, the numerical evidence suggests otherwise, for the magnitude of $(\theta - \phi)$ decreases as H increases, so that all terms in those equations remain of the same order of magnitude. The present problem is a regular perturbation problem and its analysis commences by solving for ϕ in terms of θ using Eq. (15c) recursively:

$$\phi = \theta + \frac{\phi''}{H\gamma} = \theta + \frac{\phi''}{H\gamma} + \frac{\phi''''}{(H\gamma)^2} = \ldots = \theta + \frac{\phi''}{H\gamma} + \frac{\phi''''}{(H\gamma)^2} + \frac{\phi''''''}{(H\gamma)^3} + \ldots \quad (19)$$

Substitution for ϕ into (15b) yields

$$\left(1+\frac{1}{\gamma}\right)\theta'' + f\theta' = -\frac{1}{\gamma}\left[\frac{\theta''''}{H\gamma} + \frac{\theta''''''}{(H\gamma)^2} + \ldots\right], \quad (20)$$

which, together with Eq. (15a), may be solved using a series expansion in inverse powers of H. The first two terms in this series may be written in the form,

$$f = \left(1+\frac{1}{\gamma}\right)^{1/2}\left[f_0(\zeta) + \frac{f_1(\zeta)}{(1+\gamma)^2 H} + \ldots\right], \qquad \theta = \theta_0(\zeta) + \frac{\theta_1(\zeta)}{(1+\gamma)^2 H} + \ldots, \quad (21)$$

where

$$y = \left(1+\frac{1}{\gamma}\right)^{1/2}\zeta, \quad (22)$$

and where the coefficient functions in (21) satisfy

$$f_0' = \theta_0,\ \theta_0'' + f_0\theta_0' = 0, \quad (23)$$

$$f_0' = \theta_1,\quad \theta_1'' + f_0\theta_1' + f_1\theta_0' = -\theta_0'''' = \theta_0'[F_0^3 - 3F_0\theta_0 + \theta_0'], \quad (24)$$

Solutions of these equations subject to the appropriate boundary conditions were undertaken using a fourth order Runge-Kutta shooting method code, and the resolution was such that more than 4-digit accuracy was obtained.Therefore the surface rates of heat transfer for the two phases are given by

$$\left.\frac{d\theta}{dy}\right|_{y=0} = \left(1+\frac{1}{\gamma}\right)^{-1/2}\left[\theta_0'(0) + \frac{\theta_1'(0)}{(1+\gamma)^2 H} + \ldots\right] \quad (25)$$

$$\left.\frac{d\phi}{dy}\right|_{y=0} = \left(1+\frac{1}{\gamma}\right)^{-1/2}\left[\theta_0'(0) + \left(\frac{\theta_1'(0)}{(1+\gamma)^2} + \frac{\theta_0'(0)}{(1+\gamma)}\right)\frac{1}{H} + \ldots\right], \quad (26)$$

where $\theta'_0(0) \cong -0.62755$ and $\theta'_1(0) \cong -0.46360$. These curves are plotted in Fig. 1 where excellent agreement with the fully numerical solution is seen. There is no *a priori* reason why the series expansions (21) should not continue as a regular perturbation expansion, but the computation of further terms becomes rapidly more complicated.

Asymptotic Solution for Small Values of *H*

The structure of the large-H asymptotic analysis follows closely the boundary layer analysis of [7] at large distances from the leading edge, and therefore we will not present the full details of the present working. When H is small, the flow splits into two regimes, an inner layer where y = O(1), and an outer layer, where y = O($H^{-1/2}$). For ease of presentation we set

$$\varepsilon = H^{1/2} \text{ and } \eta = y/\varepsilon. \tag{27}$$

If we denote f, θ and φ by F, Θ and Φ in the outer layer, then the inner layer equations are

$$f' = \theta, \quad \theta'' + f\theta' = \varepsilon^2(\theta - \phi), \quad \phi' = \varepsilon^2\gamma(\phi - \theta) \tag{28}$$

and the outer layer equations are

$$\Theta = \varepsilon F', \quad F\Theta' = \varepsilon(\Theta - \Phi - \Theta''), \quad \Phi'' - \gamma\Phi = -\gamma\Theta, \tag{29}$$

where primes denote derivatives with respect to y in the inner layer, and η in the outer layer. The analysis proceeds by expanding the solutions of(28) and (29) in power series in ε:

$$(f, \theta, \phi) = (f_0, \theta_0, \phi_0) + \varepsilon(f_1, \theta_1, \phi_1) + \varepsilon^2(f_2, \theta_2, \phi_2) + \ldots, \tag{30}$$

$$(F, \Theta, \Phi) = (F_0, \Theta_0, \Phi_0) + \varepsilon(F_1, \Theta_1, \Phi_1) + \varepsilon^2(F_2, \Theta_2, \Phi_2) + \ldots, \tag{31}$$

solving each set of equations in turn at increasing powers of ε, and using the method of matched asymptotic expansions. At O(1) in the inner layer we find that

$$f_0' = \theta_0, \qquad \theta_0'' + f_0\theta_0' = 0, \qquad \phi_0'' = 0, \tag{32a, b, c}$$

subject to $f_0(0) = 0$, $\theta_0(0) = 1$, $\phi_0(0) = 1$ and θ_0, $\phi_0' \to 0$ as $y \to \infty$. Clearly $\phi_0 = 1$ which implies the existence of an outer layer, for we should recover $\phi \to 0$ at sufficiently large distances from the surface. Equations (32a) and (32b) may be reduced to those of Cheng & Minkowycz [8] for the free convective boundary layer flow from a constant temperature vertical surface in a porous medium. The asymptotic value of f_0 is

$$\lim_{y\to\infty} f_0 = 1.61612/\sqrt{2} = 1.14277 \equiv A_0 \tag{33}$$

and θ_0 becomes exponentially small at large values of y.

The leading-order outer-layer equations are

$$\Theta_0 = 0, \quad F_0\Theta_0' = 0, \quad \Phi_0'' - \gamma\Phi_0 = -\gamma\Theta_0 \tag{34}$$

from which we find that

$$\Theta_0 = 0, \quad \Phi_0 = e^{-\gamma^{1/2}\eta}, \tag{35 a, b}$$

and F_0 is unknown at present. At O(ε) in the outer layer we have

$$F_0' = \Theta_1, \qquad F_0\Theta_1' = -\Phi_0, \qquad \Phi_1'' - \gamma\Phi_1 = -\gamma\Theta_1. \tag{36a, b, c}$$

Equations (36a) and (36b) may be combined to yield

$$F_0F_0'' = -e^{-\gamma^{1/2}\eta} \tag{37}$$

subject to $F_0(0) = A_0$ and $F_0' \to 0$ as $\eta \to \infty$, where the $\eta = 0$ boundary conditions was obtained using the asymptotic matching principle. Numerical solutions of Eq. (37) are depicted in Fig. 2 for various values of γ. The value of $F_0'(0)$ will be required later, and we denote its value by A_1. Equation (36c) may be solved using the particular integral and complementary function method: let

$$\Phi_1 = \widetilde{\Phi}_1 + Ce^{-\gamma^{1/2}\eta} \tag{38}$$

where C is a constant to be found and where $\widetilde{\Phi}_1(0)$ and $\widetilde{\Phi}_1 \to \infty$ as $\eta \to \infty$. We denote the resulting values of $\widetilde{\Phi}_1'(0)$ by A_2. At $O(\varepsilon)$ in the inner region the equations are

$$f_1' = \theta_1, \quad \theta_1'' + f_1\theta_0' + f_0\theta_1' = 0, \quad \phi_1'' = 0, \tag{39a, b, c}$$

subject to $f_1(0) = \theta_1(0) = \phi_1(0) = 0$ and both $\theta_1 \to A_1$ and $\phi_1 \to -\gamma^{1/2}$ as $y \to \infty$.
Clearly

$$\phi_1 = -\gamma^{1/2} y \tag{40}$$

and the solutions of (39a) and (39b) are obtained numerically. Asymptotic matching between ϕ and Φ shows that C = 0 in (38). We define A_3 as the value of $\lim_{y\to\infty}(f_1 - A_1 y)$. As in the previous section all the ordinary differential equations were solved using the fourth order Runge-Kutta method. The surface rates of heat transfer for the two phases are now given by

$$\theta'(0) = \theta_0'(0) + \varepsilon\theta_1'(0) + \ldots, \tag{41}$$

$$\phi'(0) = \; + \varepsilon[-\gamma^{1/2}] + \ldots, \tag{42}$$

where $\theta_0'(0) = -0.62756$ and the coefficient of ε in Eq. (41) is given in Table 1. The asymptotic rates of heat transfer given by (41) and (42) turn out to be valid only for very small values of H, but further improvement by including the next terms in the asymptotic expansion cannot be given explicitly because the inner-layer equations yield eigensolutions at $O(\varepsilon^2)$.

TABLE 1.
Values of $\theta_1'(0)$ as a Function of γ.

γ	$\theta_1'(0)$
0.1	0.5272
0.2	0.4527
0.5	0.3547
1.0	0.2842
2.0	0.2201
5.0	0.1501
10.0	0.1094

Discussion

We have considered in detail the free convective stagnation point flow in a porous medium using a thermal nonequilibrium model by undertaking a numerical study and performing

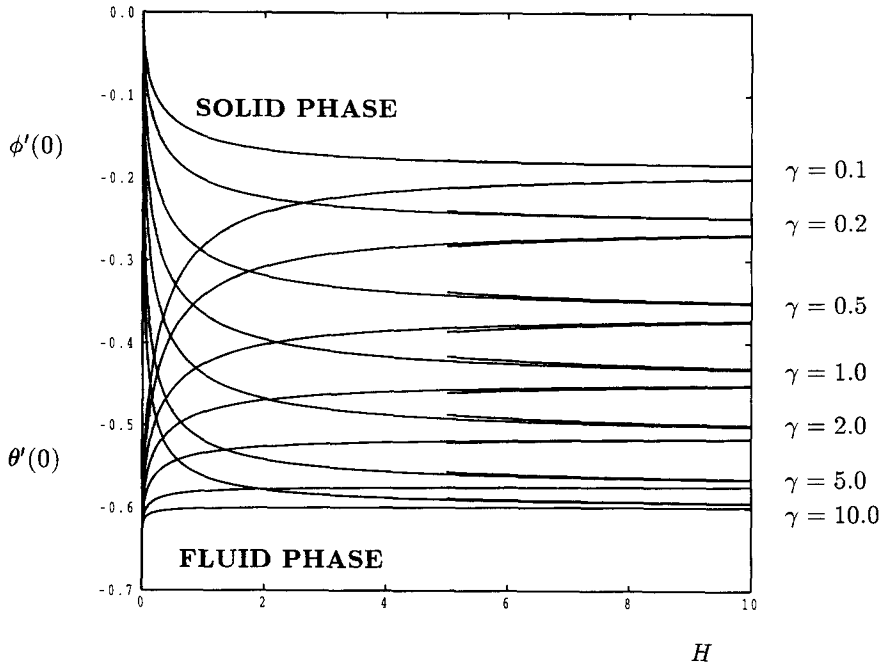

FIG. 1
Variation of $\theta'(0)$ and $\phi'(0)$ with H as obtained from solving Eqs. (15)

two asymptotic analysis. When H is small the inter-phase heat transfer is very poor allowing the solid phase temperature to conduct well away from the heated surface and to occupy a region which, at analysis. When H is small the inter-phase heat transfer is very poor allowing the solid phase temperature to conduct well away from the heated surface and to occupy a region which, at leading order is much larger than that of the fluid phase. Thus nonequilibrium effects are very strong when H is small. As H increases the heat transfer between the phases occurs more readily and this is reflected by the increasing similarity between the surface rates of heat transfer of the phase. For large values of H we have almost recovered the thermal equilibrium case where the fluid and solid temperature fields are identical. Indeed we have shown that the difference between the detailed profiles is proportional to H^{-1}. Variations in γ have not been investigated as thoroughly, but they have the same qualitative effect as variations in H. This is seen clearly in (i) Fig. 1, where large values of γ reduce nonequilibrium effects, (ii) the results of the large-H analysis given in (25) and (26) where the difference between the surface rates of heat transfer decreases as γ increases, and (iii) the small-H analysis where the thickness of the outer region (which is proportional to $\gamma^{-1/2}$ - see Eq. (35b)), which is a measure of nonequilibrium effects, decreases as γ increases.

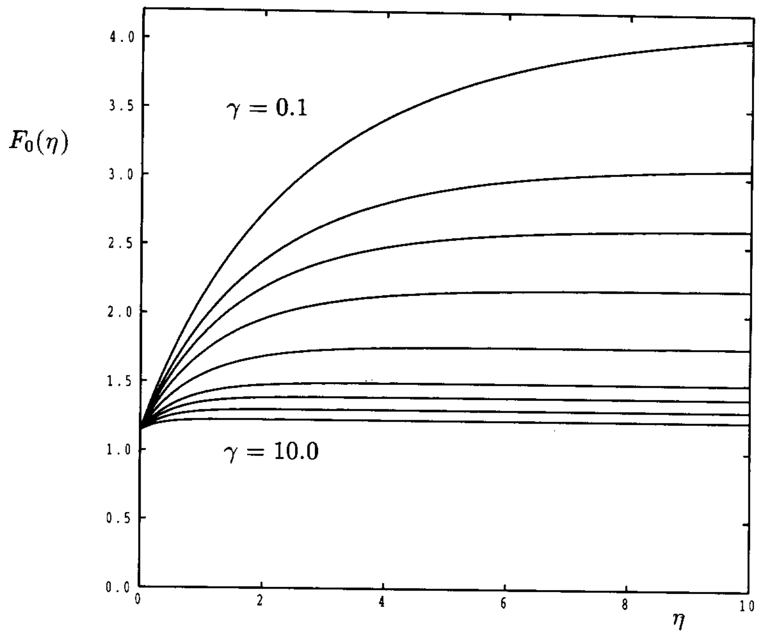

FIG. 2
Profiles of $F_0(\eta)$ as obtained by solving Eq.(37).
The values of γ are: 0.1, 0.2, 0.3, 0.5, 1.0, 2.0, 3.0, 5.0 and 10.0

References

1. D.A. Nield and A. Bejan, *Convection in Porous Media(2nd edition)*. Springer, New York (1998).

2. D.B. Ingham and I. Pop (eds.), *Transport Phenomena in a Porous Media*. Pergamon, Oxford (1998).

3. M. Combarnous, C.R. Acad.Sci. Paris A275, 1375 (1972).

4. M. Combarnous and S. Bories, Int.J.Heat Mass Transfer17, 505 (1974).

5. A.V. Kuznetsov, *Thermal nonequilibrium forced convection in porous media*. In Transport Phenomena in Porous Media, pp.103-130 (D.B. Ingham and I. Pop, eds.). Pergamon, Oxford (1998).

6. K. Vafai and A. Amiri, *Non-Darcian effects in confined forced convective flows*. In Transport Phenomena in Porous Media, pp.313-329 (D.B. Ingham and I. Pop, eds.). Pergamon, Oxford

(1998).

7. D.A.S. Rees and I. Pop, *Vertical free convective boundary-layer flow in a porous medium using a thermal nonequilibrium model.* To appear in Journal of Porous Media

8. P. Cheng and W.J. Minkowycz, J. Geophys. Res. 82, 2040 (1977).

9. D.A.S. Rees, Free convective boundary-layer flow from a heated surface in a layered porous medium. To appear in J. Porous Media.

Received May 31, 1999